European Commission | Horizon 2020 European Union funding for Research & Innovation

Horizon 2020 Grant Agreement Number 734798

indoor small-cell Networks with 3D MIMO Array Antennas (is3DMIMO)

D3.1
Report on indoor 3D MIMO interference modelling and analysis

Authors(s)	Hui Zheng, Haonan Hu and Jiliang Zhang
Author(s) Affiliation	University of Sheffield, UK; Lanzhou University, China
Editor(s):	Xiaoli Chu and Jie Zhang
Status-Version:	Final-version
Project Number:	734798
Project Title:	indoor small-cell Networks with 3D MIMO Array Antennas (is3DMIMO)
Project Acronym:	is3DMIMO
Work Package Number	3

Abstract
The three-dimension (3D) multiple-input multiple-output (MIMO) array antennas have been proposed to reduce the inter-cell interference in cellular networks by adjusting the beam direction at both horizontal and vertical dimensions. To reduce the size of 3D MIMO array antennas, millimetre wave (mmWave) spectrum is desirable to be used. As the penetration losses of mmWave transmissions are much higher than those of microwave transmissions, the indoor blockages have a significant impact on the link and interference modelling in mmWave 3D MIMO indoor small-cell networks, which is fundamental for the network performance analysis. We note that the indoor blockage layouts vary significantly in different indoor environments, and the orientations and lengths of indoor blockages may have physical influences on signal transmissions. Accordingly, conventional measurement-based methods (e.g., ray-launching based and ray-tracing based methods) would be inapplicable for statistical interference modelling for general indoor environments with random indoor blockage layouts. Stochastic geometry has been widely used in the interference modelling for large-scale randomly-deployed outdoor heterogeneous networks, but has not been sufficiently exploited for indoor MIMO small-cell (SC) networks. In this report, we investigate the interference modelling for a single-floor densely deployed indoor SC network with randomly located interior walls under the stochastic-geometry framework. The interior wall blockages are modelled as a random process of straight lines in a two-dimension (2D) plane. The centres of the straight lines are distributed following a Poisson point process (PPP), their orientations are limited in two orthogonal directions in a 2D plane with equal probabilities, and their lengths follow a uniform distribution in a certain range. Based on this stochastic wall model, the line-of-sight (LOS) and none-LOS (NLOS) probabilities for an arbitrary link in the indoor SC network are obtained. By combining the LOS and NLOS probabilities with the log-distance path loss model and the Rayleigh small-scale fading, we derive the probability distribution of the aggregate interference power received by a typical user equipment (UE) that locates at the centre of the single-floor indoor network model. Based on the obtained distribution, the coverage probability of the typical UE is derived and validated by Monte Carlo simulations. The numerical results indicate that there exits an optimal SC base station (BS) density for maximizing the coverage probability of the typical UE, and this optimal SC-BS density is dependent on the interior blockage density. The indoor SC network interference model obtained in this report will be extended to a 3D indoor SC network in conjunction with the 3D MIMO antenna patterns designed in Work Package 2 to provide fundamental understanding of the network performance gains achievable from the dense deployment of 3D MIMO SCs in 3D indoor environments.

Keywords: Millimetre wave, Interference modelling, Indoor, Small cell networks

Table of Contents

1 Introduction

The mobile traffic demand is increasing exponentially with the growing number of mobile devices. According to [1], the majority (80%) of the mobile traffic demand occurs indoors. The traditional solution where indoor wireless communications are served by outdoor base stations will no longer be able to meet such a huge demand [2]. Consequently, the ultra-dense deployment of indoor small-cell (SC) networks has been proposed to increase the indoor network capacity. However, the ultra-dense deployment of indoor SCs will also increase the inter-cell interference. Therefore, three-dimensional (3D) multiple input multiple output (MIMO) array antennas have been proposed to reduce the inter-cell interference in dense cellular networks by adjusting the beam direction at both the horizontal and vertical dimensions. To reduce the size of 3D MIMO array antennas, millimetre wave (mmWave) spectrum becomes desirable to be used. The mmWave communication has also been considered as one of the promising techniques to enhance the indoor network capacity in the forthcoming 5G networks by providing extra unlicensed spectrum resources [3].

As the penetration losses of mmWave transmissions are much severer than those of microwave transmissions, the indoor blockages (e.g., wall blockages, furniture, human bodies) will have a significant impact on the interference modelling for indoor mmWave SC networks [4], which makes it difficult to accurately predict the network performance [5], such as coverage probability. The indoor blockage effects are dominated by the interior wall blockages due to potentially dense interior walls located in indoor environments. Conventionally, the effects of blockages are incorporated into the log-normal shadowing model based on measurements, along with the effects of diffraction, reflection, and scattering [6]. However, the measurement based approach has some inherent drawbacks. Firstly, the empirical operation of measurement devices is required for establishing the model. This not only limits its general applicability but also ignores the specific characteristics of scenarios, including the various lengths and densities of interior walls [7]. Secondly, the distance dependency of wall-blockage effects is not captured by the measurement based approach [8]. Indeed, the longer link length is likely blocked by more interior wall blockages, resulting in severer shadow fading experienced by the indoor transmission [9].

Recently, the concepts and tools from random shape theory have been utilized to generate blockage models without the need of environmental specific data [10]. As a branch of stochastic geometry, random shape theory models the blockages in wireless cellular networks as random processes [11, 12]. In [9], the authors investigated the effects of outdoor blockages by further modelling the buildings as a random project process. The buildings were assumed as rectangles with random positions and orientations. Although it established a theory to model blockages aiming for the accurate performance estimation of networks, it was developed for urban outdoor environments only. Additionally, the assumption of random blockage orientations sacrifices the characteristics of realistic layout of interior wall blockages, which are usually vertical and horizontal in reality (e.g., ceilings and floors). Hence, the blockage model proposed in [9] is not particularly suitable for analysing indoor wireless communications.

Furthermore, in [2, 7, 13], the authors extended the stochastic outdoor blockage model to indoor environments. The authors in [2, 7] established the indoor wall blockage model by randomly generating the walls as straight lines in a plane, of which the orientations of wall blockages are assumed in the horizontal or vertical direction in a 2D plane. However, the authors only applied the proposed model on networks with a specific arrangement of transmitters, in which there are four transmitters located at the four corners of the considered rectangular indoor scenario, respectively. This is a very limited utilization for indoor SC networks. The work in [13] presented a wall blockage model based on Poisson line process, through which a building was randomly divided into rectangular rooms. Although the authors investigated the general application of their wall blockage model on the analysis of indoor networks, they ignored the effects of distance-dependent path loss. This may result in an inaccurate estimation of network performance.

In this deliverable, we present a novel approach to accurately model the aggregated interference in indoor dense SC networks and analyse indoor network performance by considering both the effects of wall blockages and distance-dependent path loss. Firstly, by using tools from random shape theory, we model the interior wall blockages as straight lines whose centers form a PPP. In terms of the wall orientation, a 2D coordinate system is defined with the vertical and horizontal axes. By taking realistic layouts of interior walls into account, the wall orientation is assumed to be facing the horizontal or vertical axis with an equal probability. Based on the proposed interior wall blockage model, the distribution of penetration loss caused by walls on a link is derived. Then, a path loss model incorporating both the blockage-based and distance-dependent path loss is established. Finally, the composite path loss model is applied to investigate the coverage probability of a typical user equipment (UE) in indoor dense SC networks. The results indicate that there exits an optimal SC-BS density for maximizing the coverage probability of the typical UE, and this optimal SC-BS density is dependent on the interior blockage density.

The rest of the deliverable is organised as follows. The system model is illustrated in Section 2. Then the wall blockage model is presented and its analytical tractability is demonstrated, and the coverage probability for the indoor scenario with impenetrable blockages is derived in Section 3. The simulation and numerical results are presented to validate our proposed indoor blockage modelling approach and to analyse the coverage probability of indoor dense SC networks in Section 4. Section 5 presents the conclusion and furture works.

2 System Model

In this section, we introduce our system model for analysing the performance of indoor dense SC networks. We focus on the downlink propagations for a typical indoor UE, which is only served by indoor SCs. The key assumptions are presented as follows: we consider a stochastic indoor SC network, where the SC base stations form a homogeneous PPP with density μ. All SC base stations are assumed on the ground plane. The typical UE is set at the centre of the considered indoor scenario. This work only considers the indoor scenarios with rectangular shapes. A tractable Boolean scheme of straight lines is employed to generate interior wall blockages within the indoor scenario in a 2D plane. The width (thickness) of an interior wall are ignored here because the width is much smaller as compared to the length of the wall. The wall length is assumed to follow an arbitrary distribution $f_L(l)$ with the average length $E[L]$. The centres of wall blockages form an independent PPP with density λ. The orientation of each straight line (which represents an interior wall) is assumed to be a binary random variable taking the value of 0 or $\pi/2$ with an equal probability.

We employ a path loss model that incorporates both the distance-dependent and blockage-based path loss. The small scale fading is assumed as Rayleigh fading. Accordingly, the received power of the i-th link is

$$P_i = \frac{P_T h_i S_i}{d_i^\alpha}, \tag{1}$$

where P_i is the received signal power of the i-th link, the transmitted power is assumed as a constant for each SC base station, denoted by P_T, the variable h_i is the power gain of Rayleigh fading, which follows an exponentially distribution with a unit mean, denoted by $h \sim \exp(1)$, the variable d_i^α represents the distance-dependent path loss of the i-th link with pathloss exponent α and length d_i, and S_i is the blockage-based path loss caused by interior wall blockages on the i-th link. The thermal noise is neglected hereafter for analytical tractability.

3 Coverage Performance Analysis

This section will demonstrate the effects of interior wall blockages and the coverage probability of the indoor SC network with impenetrable walls. Firstly, we investigate the effects of wall blockages. Then, the connectivity between a SC base station and UE is analyzed for the case of impenetrable wall blockages. Finally, the expression of coverage probability is derived for an indoor dense SC network considering impenetrable interior wall blockages.

3.1 The Effects of Wall Blockages

The signal power attenuation ratio caused by wall blockages of the i-th link is presented as $S_i = \prod_{k=1}^{K_i} \omega_{i,k}$, where the variable K_i denotes the number of interior walls that the i-th ($i \in Z^+$) link intersects, and $\omega_{i,k}$ denotes the attenuation caused by the k-th ($1 \leq k \leq K_i$) wall to the i-th link. Note that the value range of the variable $\omega_{i,k}$ is $[0, 1]$. For simplicity, we assume that all the interior walls have the same attenuation, i.e., $\omega_{i,k} = \omega$, hence $S_i = \prod_{k=1}^{K_i} \omega$. Therefore, it is necessary to identify statistical distribution for the number of interior walls first.

As mentioned in Section 2, we assume that the orientation angles of wall blockages are binary random variables taking values in the set $\left\{0, \frac{\pi}{2}\right\}$ with equal probabilities. Based on the system model and the assumptions of walls in Section 2, the average number of interior walls that each link intersects can be calculated following Theorem 1.

Theorem 1. *Under the assumption that the wall orientation angle takes value in the set of* $\left\{0, \frac{\pi}{2}\right\}$ *with an equal probability, the average number of interior walls that the i-th link intersects can be calculated as*

$$E[K_i] = \frac{1}{2} \left(|\sin(\varphi_i)| + |\cos(\varphi_i)| \right) \lambda E\left[L\right] d_i \tag{2}$$

where φ_i is the angle between the i-th link and the horizontal axis. It is uniformly distributed in $(0, 2\pi]$. The variable d_i denotes the length of the i-th link. The variables λ and $E\left[L\right]$ are the density and the average length of walls, respectively.

Proof. As shown in Fig. 1, the i-th link is intersected by the wall if and only if its center falls into the parallelogram region $ABCD$ (or $MNQP$). The number of walls that the i-th link intersects is equal to the number of wall-centre points falling into the region, which is given by $K_i = \lambda l_i d_i \left|\sin \gamma_i\right|$. We define the variable γ_i as the angle between a wall and the i-th link, which is uniformly distributed in $[0, \pi]$.

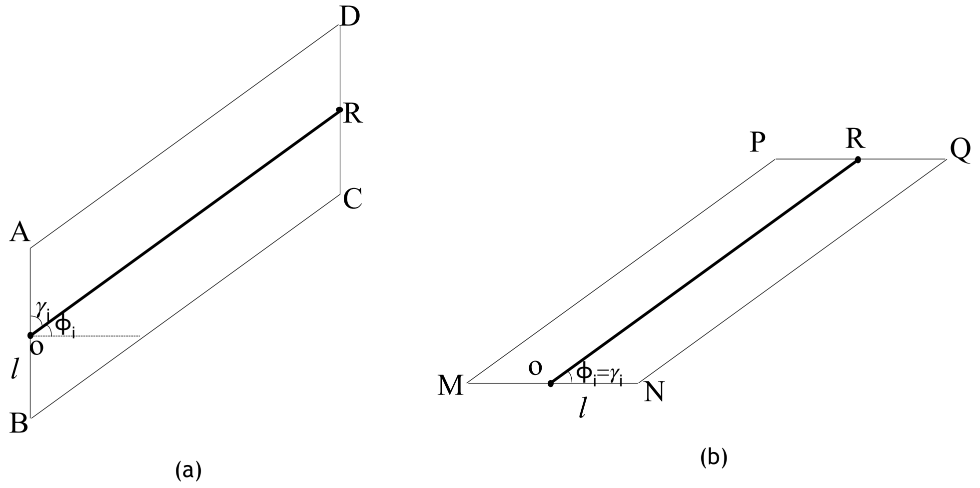

Figure 1: OR represents the i-th link with length d_i. $|AB|$ and $|CD|$ are two examples of walls each with the vertical orientation angle, denoted by $\theta = \frac{\pi}{2}$. $|MN|$ and $|PQ|$ are two examples of walls each with an horizontal orientation angle, denoted by $\theta = 0$. The variable γ_i is the angle between a wall and the i-th link, and the variable ϕ_i denotes the angle between the horizontal axis and the i-th link. The points O and R represent the positions of the typical UE and the base station, respectively. (a) An example with the wall orientation angle $\theta = \frac{\pi}{2}$. (b) An example with the wall orientation angle $\theta = 0$.

Under the assumption of wall orientation in Section 2, the orientation angle of the wall blockage is denoted by $\theta = 0$ or $\frac{\pi}{2}$. For $\varphi_i \in \left(0, \frac{\pi}{2}\right]$, we can obtain the relationship between γ_i and φ_i from Fig. 1, given by

$$\gamma_i = \begin{cases} \frac{\pi}{2} - \varphi_i, & when\ \theta = \frac{\pi}{2}, \\ \varphi_i, & when\ \theta = 0. \end{cases} \tag{3}$$

Therefore, the probability density function (PDF) $f_\Gamma(\gamma_i)$ of γ_i is given by

$$f_\Gamma(\gamma_i) = \frac{1}{2}\delta[\gamma_i - (\frac{\pi}{2} - \varphi_i)] + \frac{1}{2}\delta[\gamma_i - \varphi_i] \tag{4}$$

where δ is Dirac function. When φ_i is within $\left(\frac{\pi}{2}, 2\pi\right]$, the function $f_\Gamma(\gamma_i)$ is the same as in equation (4). The derivation is omitted here for brevity.

Following Theorem 1 of the work [9], the expected value of K_i can be calculated

$$\begin{aligned} E\left[K_i\right] &= \int_L \int_\Gamma \lambda l_i d_i \left|\sin \gamma_i\right| f_L(l_i) f_\Gamma(\gamma_i) dl \ d\gamma \\ &= \frac{1}{2}\left(\left|\sin(\varphi_i)\right| + \left|\cos(\varphi_i)\right|\right) \lambda E\left[L\right] d_i \end{aligned} \tag{5}$$

where $f_L(l_i)$ is the probability density function of the length of an interior wall. □

According to the independent thinning, the number of points falling into the region $ABCD$ (or $MNQP$) is still a PPP [14]. Moreover, Theorem 1 provides the average number of wall blockages on each link. Therefore, we can obtain that the number K_i of walls intersected by the i-link is a Poisson random variable with a mean $E[K_i]$.

As aforementioned, the attenuation is expressed as $S_i = \prod_{k=0}^{K_i} \omega$, where K_i is the number of walls intersected by the i-th link. Now with the distribution of the number of interior walls intersected by the i-th link, the signal attenuation caused by wall blockages to the i-th link can be investigated.

Based on the signal attenuation S_i caused by interior wall blockages, we analyse the performance of indoor wireless networks. In the following, we will investigate the case of mmWave networks, since wireless transmissions in this frequency range are particularly sensitive to blockages. For the simplicity of analysis, we assume that the wall blockages are impenetrable, i.e., the worst case scenario for wireless signal propagation. In this case, a UE is only connected to the SC base stations with LOS links (namely visible transmitters). With impenetrable wall blockages, the signal attenuation ratio caused by wall blockages can be modeled as a Bernoulli random variable according to whether the link is blocked or not.

Corollary 1. *For millimetre wave signals, in indoor environments, the wall blockages are assumed as impenetrable. The signal attenuation ratio S_i is a Bernoulli random variable. The conditional probability of $S_i = 1$ is presented as $P\left\{S_i = 1 | \varphi_i\right\} = e^{-\lambda E[L] d_i \beta(\varphi_i)}$, where $\beta(\varphi_i) = \frac{1}{2}\left(\left|\sin(\varphi_i)\right| + \left|\cos(\varphi_i)\right|\right)$.*

The proof is straightforward and is omitted here. According to Corollary 1, it is conveniently to obtain the conditional probability of a wireless link experiencing LOS propagation in indoor environments with interior wall blockages.

Corollary 2. *In indoor environments with interior wall blockages, the probability that the i-th link is LOS is given by $P_{LOS} = e^{-\lambda E[L] d_i \beta(\varphi_i)}$.*

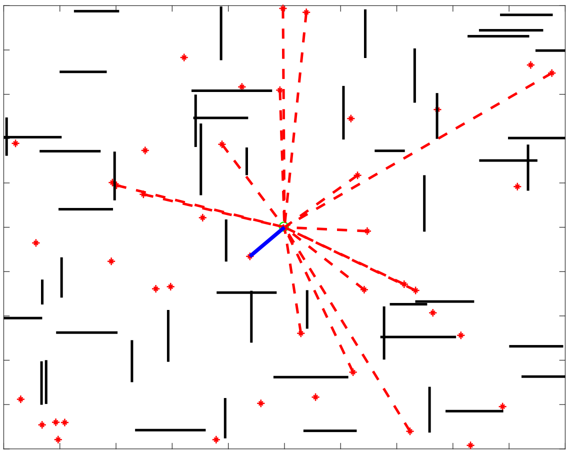

Figure 2: The wall blockages are generated as the black straight lines. All the small cell base stations are presented by the red points. The typical UE is located at the center of the considered square area. For the typical UE, all the LOS links are shown as the red dotted lines. Assume the UE is served by the nearest LOS small cell base stations shown as the blue solid line.

3.2 Connectivity

In this section, we will investigate the link connectivity between the UE and SC base stations. We assume that the typical UE is connected to the nearest LOS SC base station. The distance from the UE to the closest LOS SC base station is denoted by R. If there are more than one SC base stations with a distance R to the UE, then the UE randomly selects one of them to connect to. An example of the link connectivity is shown as in Fig. 2.

Now, we define a 3D sphere $B(O, r)$, where the radius r is less than R and the center O is the typical UE's position. Within the sphere, the SC base stations are distributed following a PPP with the mean of $\pi r^2 \mu$ [14], where μ denotes the density of base stations. we define the event $E_1 = \{\text{There are } n \text{ SC base stations within the sphere } B(\mathrm{O}, \mathrm{r}).\}$, where $\mathrm{n} = 0,\ 1,\ 2,\ ...$, then the probability $P(E_1)$ of event E_1 is given by

$$P(E_1) = \frac{e^{-\pi r^2 \mu}(\pi r^2 \mu)^n}{n!}. \tag{6}$$

The necessary and sufficient condition of a successful connectivity for the typical UE is that all the n SC base stations within the above defined sphere are not visible to the typical UE. We define the event as $E_2 = \{\text{All the } n \text{ SC base stations within the sphere } B(\mathrm{O}, \mathrm{r}) \text{ are not visible to the typical UE.}\}$. The conditional probability of event E_2 is the probability that all the n SC base stations are non-line-of-sight (NLOS) to the typical UE under the condition of event E_1. The conditional probability $P(E_2)$ of event E_2 is given by

$$\begin{aligned} P(E_2|E_1) &= \left[\int_0^{2\pi}\int_0^{r}(1-P_{LOS})\frac{2t}{r^2}\frac{1}{2\pi}\mathrm{d}t\mathrm{d}\varphi_i\right]^n \\ &= \left[1-\frac{2}{r^2}\int_0^{2\pi}M[\beta(\varphi_i)]\frac{1}{2\pi}\mathrm{d}\varphi_i\right]^n, \end{aligned} \tag{7}$$

where $M[\beta(\varphi_i)] = \frac{1-\{\beta(\varphi_i)E[L]\lambda r+1\}e^{-\beta(\varphi_i)E[L]\lambda r}}{\{\beta(\varphi_i)E[L]\lambda\}^2}$, and P_{LOS} is obtained from Corollary 2. Equation (7) follows the fact that all points in the sphere are independent and uniformly distributed according to a PPP. The link angle φ_i is uniformly distributed in $(0, 2\pi]$. The blockages that intersect each individual link are assumed to be independent.

Following Theorem 8 of the work in [9], the distribution of the distance from the typical UE to the nearest visible SC base station is obtained as

$$\begin{aligned} P(R>r) &= P(E_2) = \sum_{n=0}^{\infty}P(E_2|E_1)P(E_1) \\ &= \sum_{n=0}^{\infty}\left[1-\frac{2}{r^2}\int_0^{2\pi}M[\beta(\varphi_i)]\frac{1}{2\pi}\mathrm{d}\varphi_i\right]^n\frac{e^{-\pi r^2\mu}(\pi r^2\mu)^n}{n!} \\ &= e^{-2\pi\mu\left[\int_0^{2\pi}M[\beta(\varphi_i)]\frac{1}{2\pi}\mathrm{d}\varphi_i\right]} \\ &\overset{(a)}{\approx} e^{-2\pi\mu M\left[\mathbb{E}_{\varphi_i}[\beta(\varphi_i)]\right]} \\ &= e^{-2\pi\mu M[\widetilde{\beta}]}, \end{aligned} \tag{8}$$

where $\widetilde{\beta} = \int_0^{2\pi}\beta(\varphi_i)\frac{1}{2\pi}\mathrm{d}\varphi_i = \frac{2}{\pi}$ is the expected value of $\beta(\varphi_i)$. In step (a), we take an approximation in order to obtain a closed form expression and $M[\widetilde{\beta}] = \frac{1-\left\{\widetilde{\beta}E[L]\lambda r+1\right\}e^{-\widetilde{\beta}E[L]\lambda r}}{\left\{\widetilde{\beta}E[L]\lambda\right\}^2}$.

Following equation (8), the probability density function of R can be calculated directly by differentiation, as presented in Theorem 2.

Theorem 2. *The typical UE is connected to one of the nearest visible small cell base stations at a distance R away from the typical UE. The probability density function of R is given by*

$$f_R(r) = 2\pi\mu r e^{-[2\pi\mu M[\widetilde{\beta}]+E[L]\lambda r\widetilde{\beta}]} \tag{9}$$

Proof. Equation (9) is obtained by differentiating $1-P(R>r)$ with respect to r, which is omitted here for brevity. □

3.3 Coverage Probability

The coverage probability $P_c(T)$ is defined as the probability that the signal-to-interference ratio (SIR) received at the typical UE is larger than the threshold T, i.e.,

$$P_c(T) = P(\text{SIR} > T). \tag{10}$$

The coverage probability is an important metric for the analysis of network performance, which is influenced by the density of SC base stations, and the density and topology of interior walls. Moreover, another influential factor is the user-cell association strategy for a UE to select a SC base station to connect to. Usually a UE is connected to the SC base station with the strongest downlink received power or the maximum received SIR. We assume that the typical UE is served by the nearest visible SC base station, which is referred to as the serving base station. The downlink transmissions from other BSs are considered as interference to the typical UE. If there is no visible SC base station to the UE, then the UE is not covered, i.e., without a successful connectivity. For analytical simplicity, we assume that the number of wall blockages on each individual link is independent. The coverage probability is given in Theorem 3.

Theorem 3. *The typical UE selects the nearest visible SC base station as its serving base station. Assuming that the number of wall blockages on each link is independent and the SIR threshold is T, then the coverage probability $P_c(T)$ is given by*

$$P_c(T) = \int_0^D \exp\left(-2\pi\mu \int_r^\infty \left[\frac{Tr^\alpha e^{-\lambda E[L] t \widetilde{\beta}}}{t^\alpha + Tr^\alpha}\right] t\mathrm{d}t\right) f_R(r)\mathrm{d}r, \tag{11}$$

where $\widetilde{\beta} = \frac{2}{\pi}$, and the parameter D is the maximum link length within an indoor scenario.

Proof. According to the pathloss model described in Section 2, the downlink SIR of the typical UE can be presented as

$$\text{SIR} = \frac{h_j S_j r^{-a}}{\sum\limits_{i \in \{Z\}/j, d_i \in (0,D)} h_i S_i d_i^{-\alpha}}, \tag{12}$$

where the j-th link is the successful connectivity from the nearest visible SC base station to the typical UE given that the distance from the typical UE to the closest visible SC base station is $R = r$. The variable d_i is the length of the i-th link, and $r < d_i < D$. The variable D denotes the maximum length of links within the indoor scenario, and is defined as $D = \frac{\sqrt{{L_s}^2 + {W_s}^2}}{2}$, in which the parameters of L_s and W_s are the length and width of the indoor scenario, respectively. For improving the accuracy of analysis, the value of link length d_i is taken according to the specific indoor scenario size. The variable S_i is the wall signal attenuation ratio of the i-th link. The fading power loss denoted by h_i (and h_j) is following a unit-mean exponential distribution.

Therefore, the coverage probability conditioned on the distance from the typical UE to the closest SC base station is computed as

$$\begin{aligned}
&P\left\{\mathrm{SIR} > T \mid R = r\right\} = P\left\{h_j > \left(\sum_{i\in\{Z\}/j, d_i\in(0,D)} h_i S_i d_i^{-\alpha}\right) T r^{\alpha}\right\} \\
&= E\left[\exp\left(-\Big(\sum_{i\in\{Z\}/j, d_i\in(0,D)} h_i S_i d_i^{-\alpha}\Big) T r^{\alpha}\right)\right] \\
&= E\left[\prod_{i\in\{Z\}/j, d_i\in(0,D)} E_{S_i,h_i}\Big[\exp\left(-h_i S_i d_i^{-\alpha} T r^{\alpha}\right)\Big]\right] \\
&\overset{(a)}{=} E\Bigg(\prod_{i\in\{Z\}/j, d_i\in(0,D)} E_{h_i}\Big[\exp\left(-h_i d_i^{-\alpha} T r^{\alpha}\right)\Big] \\
&\qquad \int_0^{2\pi} P(S_i = 1|\varphi_i)\frac{1}{2\pi}\mathrm{d}\varphi_i + \int_0^{2\pi} P(S_i = 0|\varphi_i)\frac{1}{2\pi}\mathrm{d}\varphi_i\Bigg) \\
&\overset{(b)}{\approx} E\left(\prod_{i\in\{Z\}/j, d_i\in(0,D)} E_{h_i}\Big[\exp\left(-h_i d_i^{-\alpha} T r^{\alpha}\right)\Big] e^{-\lambda E[L] r\widetilde{\beta}} + 1 - e^{-\lambda E[L] r\widetilde{\beta}}\right) \\
&= E\left(\prod_{i\in\{Z\}/j, d_i\in(0,D)} 1 - \frac{T r^{\alpha} e^{-\lambda E[L] d_i\widetilde{\beta}}}{d_i^{\alpha} + T r^{\alpha}}\right) \\
&\overset{(c)}{=} \exp\left(-2\pi\mu \int_r^{\infty} \left[\frac{T r^{\alpha} e^{-\lambda E[L] t\widetilde{\beta}}}{t^{\alpha} + T r^{\alpha}}\right] t\mathrm{d}t\right),
\end{aligned} \tag{13}$$

where step (a) follows Corollary 1, S_i follows the Bernoulli distribution with the conditional probability of $P(S_i = 1|\varphi_i)$, step (b) takes an approximation for reducing the computing complexity, which is shown as

$$\int_0^{2\pi} P(S_i = 1|\varphi_i)\frac{1}{2\pi}\mathrm{d}\varphi_i \approx e^{-\lambda E[L] r E_{\varphi_i}[\beta(\varphi_i)]} = e^{-\lambda E[L] r\widetilde{\beta}}.$$

Step (c) is obtained from the probability generating functional (PGFL) of the PPP that models the spatial distribution of SC base stations.

Based on equation (13) and Theorem 2, the unconditional coverage probability is formulated by deconditioning the variable r as follows,

$$P\left\{\mathrm{SIR} > T\right\} = \int_0^{D} P\left\{\mathrm{SIR} > T \mid R = r\right\} f_R(r)\mathrm{d}r, \tag{14}$$

where the parameter D is the maximum link length within the considered indoor scenario, given that the typical UE is located at the centre of the considered network area as shown in Fig. 2. □

According to Theorem 3, although it is difficult to obtain the closed form expression of coverage probability, the coverage probability expression in equation (11) can be used to numerically investigate the distribution of coverage probability of indoor dense SC networks with interior wall blockages. In the next section, Theorem 3 will be employed to analyse the coverage performance of indoor cellular networks with impenetrable wall blockages.

4 Simulation Results

In this section, we present the numerical performance-evaluation results of dense cellular networks in indoor environments. Firstly, the analytical results obtained in Section 3 will be validated by comparing with Monte Carlo simulation results. Then the coverage performance of indoor dense SC networks will be analysed based on both numerical and simulation results.

We validate the average number of walls obtained in equation (2) in Theorem 1 by comparing it with Monte Carlo simulation result as shown in Fig. 3. The analytical average number of walls that each link intersects is obtained from Theorem 1. In the comparisons, we fix the link length at 20 meters and consider three different values of the average wall length $E[L]$: 3 meters, 5 meters and 7 meters. Considering that the considered network scenario is symmetric with respect to its central point (the position where the typical UE is located) as shown in Fig. 2, only the results in the interval $(0, \pi/2]$ of the angles between the links and the horizontal axis are presented here. The Monte Carlo simulation results are averaged over 10,000 samples. From Fig. 3, it is observed that the analytical results match the simulation results closely. The links with angle $\phi = 0$ or $\pi/2$ intersect the smallest number of interior walls on average. The reason is the links with angle $\phi = 0$ or $\pi/2$ are only blocked by the horizontal or vertical walls at this time, where the density of walls is only half of λ.

Fig. 4 presents a comparison of coverage probability between analytical results and Monte Carlo simulation results, under impenetrable wall blockages. The analytical results are obtained from Theorem 3 in Section 3.3. The parameter T denotes the SIR threshold. The values of the main parameters are summarised in Table **I**. From Fig. 4, we can observe that the curves of analytical results match the Monte Carlo simulation

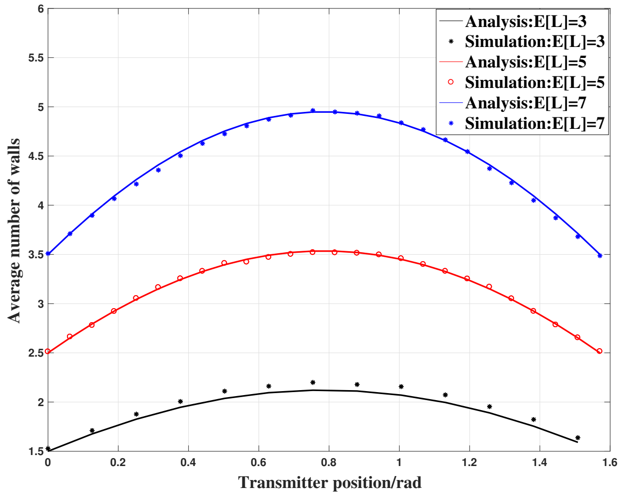

Figure 3: The validation of average wall number intersected by links. We simulate a square area of 40×40 m^2. The wall density is assumed as $\lambda = 0.05$ m^{-2}. The average wall length takes $E[L] = 3, 5, 7$ m respectively. The link length is assumed as 20 m for both the analysis and simulation. The position of typical UE is located at the centre of the scenario as shown in Fig. 2. The position of the server base station is located at the circle with the centre of UE's position and the radius of link length.

Table 1: Simulation parameters

Pathloss exponent	$\alpha = 2$
SC BS transmit power	$P = 1$W
Wall penetration loss	$\omega = 10$dB
Number of samples per simulation	10^4

results closely with only a small gap between them. The small gap is caused by the correlations of wall blockage effects on different links, which are captured in the Monte Carlo simulation but ignored in the analytical result in Theorem 3. Additionally, in stochastic geometry, the average coverage probability is derived by aggregating the SIR over the infinite 2-D plane. However, the considered indoor scenario is of a finite area. We adjust the integral limits in equation (13) according to the specific indoor scenario size, which contributes to the difference between the analytical coverage probability and the simulation result. The reasonably good accuracy of the analytical coverage probability expression in Theorem 3 (as compared with the Monte Carlo simulation result) indicates that Theorem 3 offers a good trade-off between performance evaluation (or prediction) accuracy and the computational complexity. The Monte Carlo simulation took several

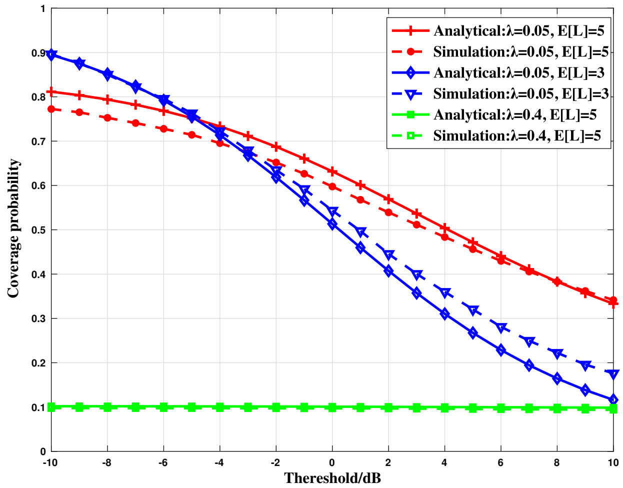

Figure 4: The verification of the coverage probability expression in (11) by comparing it with Monte Carlo simulation results. Assume the indoor scenario as a square of 40×40 m^2. Given the distribution of SC base stations with a density $\beta = 0.01$ m^{-2}, the values of wall density are taken as $\lambda = 0.01, 0.4$ m^{-2}, and average wall length are taken as $E[L] = 3, 5$ m, respectively. The typical UE is located at the center of the considered network scenario.

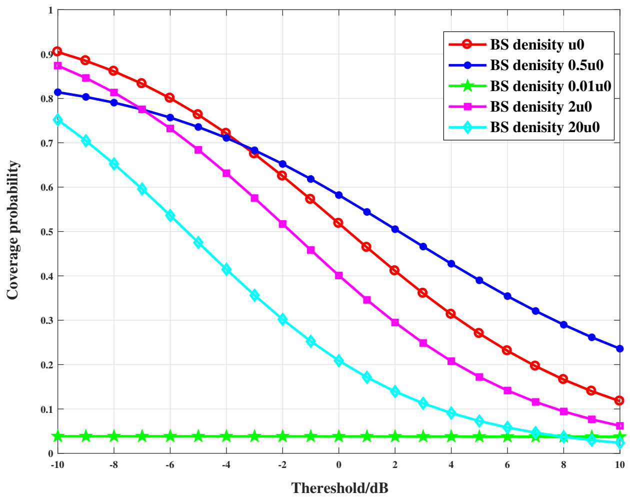

Figure 5: The coverage probability obtained as a function of transmitter density in Theorem 3 versus the SIR threshold for different values of SC base station density, given the wall density $\lambda = 0.05$ m^{-2}. The average wall length is $E[L] = 3$ m. The SC base station density is $\mu_0 = 0.01$ m^{-2}. The typical UE is located at the center of the considered indoor network scenario.

hours to complete all the calculations for 10,000 samples.

Fig. 5 presents the coverage probability calculated using equation (11) in Theorem 3 versus the SIR threshold for different values of SC base station density. An apparent observation is that the coverage probability does not always benefit from the increasing density of SC base stations, given the distribution of wall blockages in an indoor environment. In other words, for indoor dense cellular networks with interior wall blockages, there is a finite optimum density of SC base stations that maximizes the coverage probability. This is because increasing the density of SC base stations will also increase the number and density of interfering links, making the coverage probability limited by the interference. In addition, the coverage is very poor when the SC base station density is relatively low compared to the wall blockage density. This is because the typical UE can hardly find any LOS SC base station to connect to when the wall blockage density is much larger than that of SC base station density.

5 Conclusion

In this deliverable, we have investigated the interior wall blockages and the associated analysis of interference effects and coverage performance of indoor dense SC networks. The wall blockage model is developed on the basis of the stochastic geometry. The key idea is that the interior walls are stochastically modelled as straight lines. Then the effects of interior wall blockages on signal transmissions are investigated for indoor dense SC networks. An analytical expression of the coverage probability is derived for the case of impenetrable interior wall blockages. The analytical results are validated through comparisons with Monte Carlo simulation results. The numerical and simulation results show that the coverage probability of an indoor dense SC network is sensitive to dense interior wall blockages. Although the coverage probability can benefit from the increasing density of indoor SC base stations, there exists a finite optimum density of SC base stations that maximizes the network coverage probability given the distribution of interior walls. By combining the results in this deliverable with the indoor 3D MIMO channel modelling and 3D MIMO array antenna design results obtained in Work Package 1 & 2, Work Package 3 will consider the correlation of blockage effects in the modelling and analysis of indoor 3D MIMO small cell networks. Since in an finite indoor environment, the correlation of blockage effects between 3D MIMO links will be considerable. Moreover, the interior wall blockage model will be extended by considering the effects of reflection in indoor dense SC networks in conjunction with 3D MIMO array antennas.

References

[1] J. Zhang and G. D. la Roche, *Femtocells: technologies and deployment.* John Wiley & Sons, 2011.

[2] M. K. Mller, M. Taranetz, and M. Rupp, "Analyzing wireless indoor communications by blockage models," *IEEE Access*, vol. 5, pp. 2172–2186, 2017.

[3] Y. H. e. a. X. Ming, S. Mumtaz, "Millimeter wave communications for future mobile networks," *IEEE Journal on Selected Areas in Communications*, pp. 1909–1935, Sep. 2017.

[4] R. Mathur, M. Klepal, A. McGibney, and D. Pesch, "Influence of people shadowing on bit error rate of ieee802.11 2.4 ghz channel," in *1st International Symposium onWireless Communication Systems, 2004.*, Sept. 2004, pp. 448–452.

[5] Z. Pi and F. Khan, "An introduction to millimeter-wave mobile broadband systems," *IEEE Communications Magazine*, vol. 49, no. 6, pp. 101–107, June 2011.

[6] A. Goldsmith, *Wireless communications.* Cambridge university press, 2005.

[7] M. K. Mller, M. Taranetz, and M. Rupp, "Effects of wall-angle distributions in indoor wireless communications," in *2016 IEEE 17th International Workshop on Signal Processing Advances in Wireless Communications (SPAWC)*, July 2016, pp. 1–5.

[8] J. Salo, L. Vuokko, H. M. El-Sallabi, and P. Vainikainen, "An Additive Model as a Physical Basis for Shadow Fading," *IEEE Transactions on Vehicular Technology*, vol. 56, no. 1, pp. 13–26, Jan 2007.

[9] T. Bai, R. Vaze, and R. W. Heath, "Analysis of blockage effects on urban cellular networks," *IEEE Transactions on Wireless Communications*, vol. 13, no. 9, pp. 5070–5083, Sept. 2014.

[10] ——, "Using random shape theory to model blockage in random cellular networks," in *2012 International Conference on Signal Processing and Communications (SPCOM)*, July 2012, pp. 1–5.

[11] M. Berman, "Distance distributions associated with poisson processes of geometric figures," *Journal of Applied Probability*, vol. 14, no. 1, pp. 195–199, Mar. 1977.

[12] R. Cowan, "Objects arranged randomly in space: an accessible theory," *Advances in Applied Probability*, vol. 21, no. 3, pp. 543–569, Sept. 1989.

[13] J. Lee, X. Zhang, and F. Baccelli, "A 3-d spatial model for in-building wireless networks with correlated shadowing," *IEEE Transactions on Wireless Communications*, vol. 15, no. 11, pp. 7778–7793, Nov. 2016.

[14] F. Baccelli and B. Blaszczyszyn, *Stochastic Geometry and Wireless Networks, Volume I -Theory.* Hanover, MA, USA: NOW Publisher, 2009.